

Theoretical and numerical simulation study of the structure of the Hall electric field in the vicinity of the magnetic reconnection site

F. C. HUANG^{1,2}, F. S. WEI¹ and X. S. FENG¹

¹Key Laboratory for Space Weather, Chinese Academy of Sciences, PO Box 8701, 100080, Beijing, China

²Graduate School of the Chinese Academy of Sciences, 100039, Beijing, China
(fchuang@ns.spaceweather.ac.cn)

(Received 10 January 2005)

Abstract. The Hall effects are suggested to be responsible for the decoupling of electrons and ions of magnetic plasma in the process of magnetic reconnection. However, the process that ultimately causes the electrons to diffuse from the magnetic field in the very small diffusion region remains one of the main unsolved problems in magnetic reconnection theory. In this paper, the structure of the Hall electric field in the diffusion region is studied theoretically in the coordinate system located on the magnetic line. A numerical simulation result for this problem is also given. The new discovery is that electrons can be generated in the diffusion region due to the Hall effects. Therefore the role of the Hall effects in the decoupling of electrons and ions of a magnetic plasma can be clarified in the structure of the Hall electric field.

1. Introduction

Magnetic reconnection is an important physical process in the dynamics of astrophysical plasma systems for explaining explosive events such as solar flares and solar coronal mass ejections (CME; Yokoyama 2000; Hesse, 2000). Understanding how the frozen-in condition is broken down, how the magnetic lines reconnect in the frozen-in state and other correlated problems have been major issues (Drake et al. 2003). Magnetic reconnection begins in a small ‘diffusion region’, where the newly reconnected lines produce jets of plasma away from the diffusion region. The Hall magnetic field, the jets and the Hall current have recently been detected by the Geotail outside the diffusion region in the process of the magnetic reconnection (Nagai et al. 2001, 2003). The physical processes of magnetic reconnection have remained poorly understood because of the scarcity of *in situ* observations in the small diffusion region of the magnetic reconnection site (Øieroset et al. 2001; Drake et al. 2003).

It has been suggested that in the diffusion region electrons and ions of the magnetic plasma decouple when a magnetic reconnection takes place (Yamada et al. 1997; Øieroset et al. 2002). And this process of decoupling of electrons and ions in the diffusion region is suggested to be responsible for the breakdown of the frozen-in condition and the enhancement of the resistivity of magnetic plasmas (Fujimoto

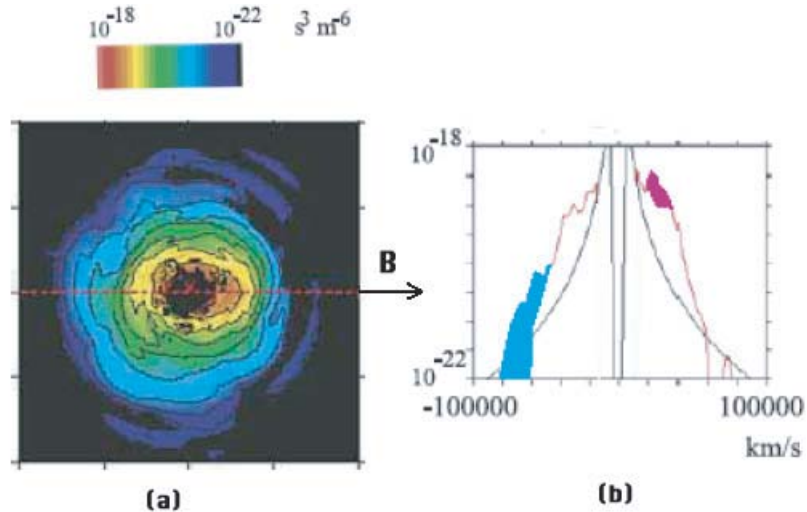


Figure 1. Electron distribution functions observed by the Geotail at 1744:00 UT, on 10 December 1996. (a) Electron phase space densities are shown in the plane that includes the magnetic field vector; (b) two electron distribution functions representing different energy-state components (Nagai et al. 2003).

2001; Vainshtein et al. 2000). In the present theories concerning the decoupling of electrons and ions in the diffusion region, the ‘Whistler-wave-driven’ model is popular, and the Hall effects play a key role in it (Deng and Mastsumoto 2001; Øieroset et al. 2001; Drake et al. 2003). In addition, the magnetic reconnection is reproduced successfully in the magnetic reconnection experiment (MRX) and in the magnetohydrodynamic (MHD) numerical simulation. However, the timescale of the magnetic reconnection in the MRX is about 300 μs , obviously far less than the timescale estimated in the MHD numerical simulation (Yamada et al. 1997; Wu et al. 2000; Ji, 2001; Cater et al. 2002; Urrutia et al. 2003). Simulating the fast magnetic reconnection is a great difficulty for the MHD simulation. In order to understand the mechanism of fast magnetic reconnection, a great deal of attention has been paid to the Hall effects recently (Vainshtein et al. 2000; Fujimoto, 2001; Ma and Lee 2001).

2. Event observed

On 10 December 1996, the observations made by Geotail obtained evidence of field-aligned current in the vicinity of the magnetic reconnection site. The current system is believed to be generated by the decoupling of ions and electrons in the magnetic plasma. The distribution functions of electrons which are in a different energetic state in the diffusion region have been obtained (Nagai et al. 2001, 2003). Two kinds of electron-distribution functions are presented in Fig. 1, observed at 1744:00 UT on 10 December 1996. We find that the maximum of the electron density is in the centre of the diffusion region, where the velocity of electrons is zero.

Outside of the diffusion region, the Hall magnetic field, jet fluids and Hall current formed during the magnetic reconnection have been observed by many spacecraft (such as Geotail and Wind). This Hall current system has been accepted by many

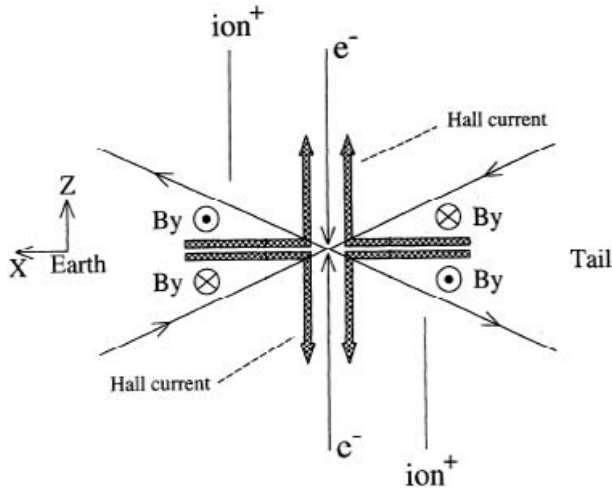


Figure 2. Sketch map of the Hall current system caused by the decoupling of electrons and ions near an X-type neutral line. Hall magnetic field B_y is also shown in this figure. Here, the illustrated plane is assumed to be the X - Z plane of the GSM coordinate system (Nagai et al. 2001).

scientists (Nagai et al. 2001, 2003; Deng et al. 2001; Øieroset et al. 2001, 2002). The distributions of electrons and ions, and the Hall current system observed by the spacecraft are shown in Fig. 2. At present, this sketch is popular in the study of magnetic reconnection.

3. The Hall term expressed in the coordinate located on the magnetic line

It is well known that there are many transient events in interplanetary space, such as shocks and magnetic clouds. The discontinuity of physical variables in the solar wind has often been observed by many spacecraft, such as Wind, Geotail and IMP8 (Horbury et al. 2001; Nagai et al. 2001). During the propagation of the disturbance, the evolution of the magnetic field has also been simulated in the numerical simulation. The result of this numerical simulation shows that the gradient of magnetic field on the neutral line of the magnetic field can become tremendous in the interaction between the disturbance and this line (Vainshtein et al. 2000). In this simulation study, the Hall term $\mathbf{J} \times \mathbf{B}/(ne)$ was taken into consideration. From these studies, it can be inferred that the Hall term in the general Ohm's law plays an important role in the region near the neutral line of the magnetic field (Vainshtein et al. 2000; Fujimoto, 2001; Ma and Lee 2001). The following discussion is based on these observational results and research conclusions.

In the coordinate system located on the magnetic line, the Hall term can be expressed as

$$\mathbf{J} \times \mathbf{B}/(ne) \quad (1)$$

where n is the density of electrons and e is the unit charge of electron.

According to Maxwell's equations, the current density can be expressed with the intensity of magnetic field, namely

$$\mathbf{J} = \nabla \times \mathbf{H} = \frac{1}{\mu_0} \nabla \times \mathbf{B}. \quad (2)$$

Inserting (2) into (1), we can obtain

$$\mathbf{J} \times \mathbf{B}/ne = \frac{1}{ne\mu_0}(\mathbf{B} \cdot \nabla)\mathbf{B} - \frac{1}{ne}\nabla\left(\frac{B^2}{2\mu_0}\right). \quad (3)$$

We will study (3) in the coordinate system located on the magnetic line. Let $\hat{\mathbf{e}}_1$, $\hat{\mathbf{e}}_2$, $\hat{\mathbf{e}}_3$ denote the unit vectors in the tangential direction, the principal normal direction and the binormal direction of the magnetic line, respectively, where $\hat{\mathbf{e}}_3 = \hat{\mathbf{e}}_1 \times \hat{\mathbf{e}}_2$. The corresponding coordinate variables are x_1 , x_2 , x_3 , respectively. In this coordinate system, the first term on the right-hand side of (3) can be expressed as (Ma et al. 1988)

$$\frac{1}{ne\mu_0}(\mathbf{B} \cdot \nabla)\mathbf{B} = \frac{1}{ne\mu_0}B\frac{\partial}{\partial x_1}(B\hat{\mathbf{e}}_1) = \frac{1}{ne\mu_0}\left[\hat{\mathbf{e}}_1\frac{\partial}{\partial x_1}\left(\frac{B^2}{2}\right) + \hat{\mathbf{e}}_2\frac{B^2}{r}\right].$$

Therefore, (1) can finally be transformed into

$$\mathbf{J} \times \mathbf{B}/(ne) = -\frac{1}{ne}\left(\hat{\mathbf{e}}_2\frac{\partial}{\partial x_2} + \hat{\mathbf{e}}_3\frac{\partial}{\partial x_3}\right)\frac{B^2}{2\mu_0} + \hat{\mathbf{e}}_2\frac{B^2}{ne\mu_0r}, \quad (4)$$

where r is the curvature radius of the magnetic line at the given point.

When the gradient of the magnetic field in the region near the neutral line of the magnetic field becomes tremendous, the last term on the right-hand side of (4) is negligible. Therefore (4) can be transformed into

$$\mathbf{J} \times \mathbf{B}/(ne) \approx -\frac{1}{ne}\left(\hat{\mathbf{e}}_2\frac{\partial}{\partial x_2} + \hat{\mathbf{e}}_3\frac{\partial}{\partial x_3}\right)\frac{B^2}{2\mu_0}. \quad (5)$$

4. The structure of the Hall electric field

When $\omega_e\tau_e \ll 1$, where ω_e is the electron gyrofrequency and τ_{ei} is the electron–proton collision time, the magnetic plasma can be taken as an ideal magnetic plasma and the Hall term in the inductive equation can be ignored, and its resistivity is zero. Thus, the plasma is frozen in the magnetic field. The frozen-in condition of magnetic field is

$$\mathbf{E} + \mathbf{u} \times \mathbf{B} = 0. \quad (6)$$

Taking the Hall term and the resistivity term into consideration, (6) should be corrected to the following equation according to the general Ohm's law (Vainshtein et al. 2000; Fujimoto 2001):

$$\mathbf{E} \approx \eta\mathbf{J} - \mathbf{u} \times \mathbf{B} + \frac{1}{ne}(\mathbf{J} \times \mathbf{B}). \quad (7)$$

Inserting (5) into (7), we can obtain the following equation:

$$\mathbf{E} \approx \eta\mathbf{J} - \mathbf{u} \times \mathbf{B} - \frac{1}{ne}\left(\hat{\mathbf{e}}_2\frac{\partial}{\partial x_2} + \hat{\mathbf{e}}_3\frac{\partial}{\partial x_3}\right)\frac{B^2}{2\mu_0}. \quad (8)$$

Let us assume

$$\mathbf{E}_{\text{Hall}} = -\frac{1}{ne}\left(\hat{\mathbf{e}}_2\frac{\partial}{\partial x_2} + \hat{\mathbf{e}}_3\frac{\partial}{\partial x_3}\right)\frac{B^2}{2\mu_0}. \quad (9)$$

Therefore, (8) can be expressed as

$$\mathbf{E} \approx \eta\mathbf{J} - \mathbf{u} \times \mathbf{B} + \mathbf{E}_{\text{Hall}}. \quad (10)$$

Based on the expression (9), the vector of the Hall electric field is perpendicular to the magnetic-field lines, and points to the site where the magnetic field is weaker from the site where the magnetic field is stronger. If this result is applied to the diffusion region of the magnetic reconnection site, we can obtain a clear picture of the structure of the Hall electric field in this region. On the neutral line of the magnetic field, the intensity of the magnetic field is zero. However around it, the intensity of the magnetic field is stronger (not zero). Therefore in the diffusion region, the vector of the Hall electric field is perpendicular to the magnetic-field line, and points to the neutral line of the magnetic field from two sides. This result can also be verified in the numerical simulation result for the magnetic reconnection given later. Some more interesting results will also be introduced from the numerical simulations.

5. Electrons can be generated in the diffusion region due to the Hall effects

A sketch of the magnetic reconnection is shown in Fig. 3. Let us take the case of a spherical Gauss surface close to the magnetic reconnection site. Gauss law can be written as

$$\oiint \mathbf{D} \cdot d\mathbf{S} = q_f \quad (11)$$

where $\mathbf{D} = \varepsilon\mathbf{E}$, q_f is the total quantity of charge in the region enclosed by the spherical Gauss surface. $\mathbf{u} \times \mathbf{B}$ is the dynamo term which leads to the frozen-in effect, having no contribution to the decoupling of ions and electrons in the magnetic plasma. Therefore, it need not be taken into account in the following discussion. (In fact, it is easy to infer that it has no contribution to the integral of (11).) Figure 3 shows the direction of the electric current density vector \mathbf{J} inside the current sheet. It comes in through the spherical Gauss surface on one side, and comes out through the spherical Gauss surface equally on the other side. Therefore, the term $\eta\mathbf{J}$ also makes no contribution to the integral of (11). Here, the Hall current (shown in Fig. 2) has not been taken into consideration. Because when the magnetic reconnection is about to take place (but has not yet taken place), there is no Hall current. So, it can be concluded that the Hall electric field is the sole term important for the integral of (11) in the diffusion region. Therefore, the integral of the electric-field intensity over the spherical Gauss surface is negative. According to Gauss's law, the total quantity of electric charge in the region enclosed by this surface is negative. And it can be inferred that the electrons are generated in the diffusion region of the magnetic reconnection site due to the Hall effects.

Of course, the conclusion obtained by us is true for the given condition. In the above discussion, the term $B^2/(\mu_0 r)$ has been ignored in the expression of the Hall electric field. It is obvious that the term $B^2/(\mu_0 r)$ (where r is the radius of curvature) is relative to the flexure of the magnetic-field line, but not related to the gradient of the magnetic field. So, the conclusion obtained by us is true for the condition when the gradient of the magnetic field is very large. The interplanetary shock is an important phenomenon, often observed by spacecrafts in interplanetary space. Owing to the interaction between the shock and the neutral line of the magnetic field, the gradient of the magnetic field in the region near the neutral line of the magnetic field is tremendous. So the conclusion obtained in this paper

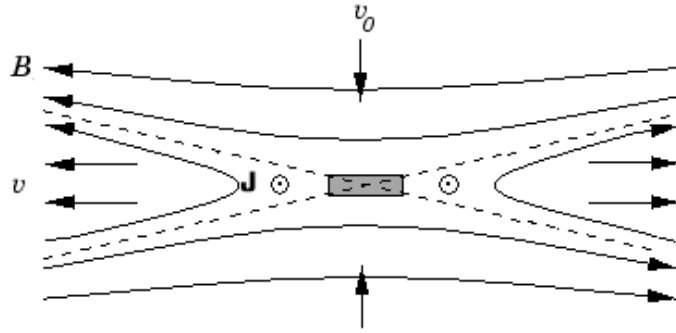


Figure 3. Sketch of the magnetic reconnection site. The electric current density \mathbf{J} , the in-flow speed v_0 and the out-flow speed v are shown in this figure. The shaded area marks the diffusion region of the magnetic reconnection site.

is true for those magnetic reconnection phenomena caused by the interplanetary shock.

However, in the present study of magnetic reconnection, for some theoretical models, such as the turbulence-driven model and the Alfvén-wave-driven model, the flexure of the magnetic-field line is an important factor and it cannot be ignored. Therefore, the conclusion obtained above by us cannot be made sure for these theoretical models.

6. Numerical simulation

In order to study the structure of the Hall electric field, the two-dimensional MHD equations are used in this numerical simulation and the inductive equation in the MHD equation is substituted by (7). The effect of the uneven distribution of the initial density of the plasma is ignored in this numerical simulation and the initial density of the plasma is assumed to be constant.

In the numerical simulation of magnetic reconnection, what is mainly of concern is the vanishing of the magnetic energy and the transferring of the magnetic flux. Therefore, the incompressible MHD equations can be used. Usually, the Hall effects are ignored in the numerical simulation of magnetic reconnection (Fu and Hu 1995). However, the gradient of the magnetic field in the region near the neutral line of the magnetic field is greater than that in other regions, especially when the disturbance interacts with the neutral line of the magnetic field, which is important for the discussion of the structure of the Hall electric field. So, the Hall term has been taken into account in this numerical simulation of magnetic reconnection.

For the sake of convenience, the vorticity $\boldsymbol{\Omega}$, the vector potential $\boldsymbol{\Psi}$ and the magnetic-field vector potential \mathbf{A} are introduced in this numerical simulation. They are defined as follows: $\boldsymbol{\Omega} = \nabla \times \mathbf{u}$, $\mathbf{u} = \nabla \times \boldsymbol{\Psi}$ and $\mathbf{B} = \nabla \times \mathbf{A}$. In the numerical simulation, we set the horizontal coordinate axis as z , the perpendicular axis as x and y is perpendicular to the surface of the sheet, pointing towards the reader. Those unit vectors on the x , y , z coordinate axes can be expressed as $\hat{\mathbf{x}}$, $\hat{\mathbf{y}}$, $\hat{\mathbf{z}}$. In the two-dimensional incompressible MHD fluid, we have

$$\frac{\partial}{\partial y} = 0, \quad B_y = u_y = 0.$$

Then, we have $\mathbf{\Omega} = \Omega \hat{\mathbf{y}}$, $\mathbf{\Psi} = \Psi \hat{\mathbf{y}}$, $\mathbf{J} = J \hat{\mathbf{y}}$, $\mathbf{A} = A \hat{\mathbf{y}}$ $\mathbf{u} = \nabla \times \mathbf{\Psi}$, $\mathbf{B} = \nabla \times \mathbf{A}$ and $\mu_0 \mathbf{J} = \nabla \times \mathbf{B}$ can be simplified to give the following expressions: $\mathbf{u} = \nabla \Psi \times \hat{\mathbf{y}}$, $\mathbf{B} = \nabla A \times \hat{\mathbf{y}}$ and $\mu_0 \mathbf{J} = \nabla B \times \hat{\mathbf{y}}$.

So, for the incompressible MHD fluid ($\gamma \rightarrow \infty$, γ is the specific heat ratio), the two-dimensional MHD dimensionless equations can be given as follows:

$$\frac{\partial A}{\partial t} = -\mathbf{u} \cdot \nabla A + \frac{1}{R_m} \nabla^2 A - \frac{m_p B_0}{e \mu_0 \mu} \cdot \frac{1}{R_n} \mathbf{B} \cdot \nabla B \tag{12a}$$

$$\frac{\partial \Omega}{\partial t} = -\mathbf{u} \cdot \nabla \Omega + \mathbf{B} \cdot \nabla J + \frac{1}{R_n} \nabla^2 \Omega \tag{12b}$$

$$\nabla^2 \Psi = -\Omega \tag{12c}$$

$$\mathbf{u} = \nabla \Psi \times \hat{\mathbf{y}} \tag{12d}$$

$$\mathbf{B} = \nabla A \times \hat{\mathbf{y}} \tag{12e}$$

$$\mu_0 J = -\nabla^2 A, \tag{12f}$$

where the dimensionless parameters R_n , R_m are, respectively, the Reynolds number and the magnetic Reynolds number:

$$R_n = \rho v_A \ell / \mu, \quad R_m = \mu_0 v_A \ell / \eta,$$

with $v_A = B_{z0} / \sqrt{\mu_0 \rho}$ being the Alfvén speed and η being the resistivity of the magnetic plasma. The sign ℓ indicates the thickness of the current sheet, the value of which will hereinafter be given in the initial magnetic field. B_0 is given as $7.9 \cdot 10^{-9}$ (T).

In the numerical simulation, the values of R_m and R_n are both 1000. ρ , μ_0 , μ , e and m_p are, respectively, the density of the magnetic plasma, the permeability of free space, the viscosity coefficient, the electronic charge and the mass of a proton. μ is taken as 1.0×10^6 Pa s, the value of which is not important for the magnetic reconnection, but is useful for computational stability. The value of m_p is 1.6726×10^{-27} kg. The third term on the right-hand side of (12a) is the Hall term corrected in this paper.

The computing area is: $-L_x \leq x \leq L_x$, $-L_z \leq z \leq L_z$ and $L_x = 2$, $L_z = 10$. The central difference format is used in the computation. The time step is limited by the CFL condition:

$$\Delta t \leq \min(\Delta x / u_x, \Delta z / u_z).$$

The boundary conditions are assumed to be as follows.

(1) On the drive boundary ($x = L_x$, $x = -L_x$):

$$\begin{aligned} u_x(x = L_x) &= -u_x(x = -L_x) = u_d(z, t) \\ B_x(x = L_x) &= -B_x(x = -L_x) = B_d(z, t) \\ \frac{\partial \Omega}{\partial x} &= 0, \end{aligned}$$

where $u_d = -0.1 c f(t) 2 / [e^{(z/L_z)} + e^{(-z/L_z)}]$, $B_d(z, t) = c f(t) \tanh(z/L_z)$ and $c = 0.00001$. $f(t)$ is given as follows: when $0 < t < 2\tau_A$, $f(t) = t / (2\tau_A)$; when $2\tau_A \leq t \leq 8\tau_A$, $f(t) = 1$; when $8\tau_A < t < 10\tau_A$, $f(t) = (10\tau_A - t) / (2\tau_A)$, where, $\tau_A = 1 / v_A$ (the Alfvén time).

(2) On the free boundary ($z = L_z$, $z = -L_z$)

$$\frac{\partial \Omega}{\partial z} = 0, \quad \frac{\partial A}{\partial z} = 0, \quad \frac{\partial \Psi}{\partial z} = 0.$$

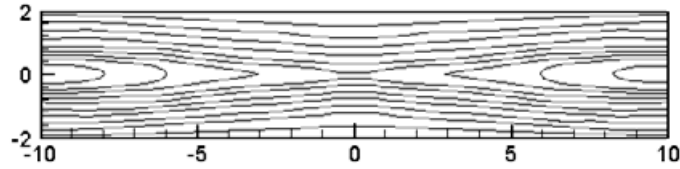


Figure 4. The simulated magnetic-line graph of magnetic reconnection ($t = 10\tau_A$).

The initial conditions are assumed to be as follows.

- (1) The initial magnetic field is assumed to be

$$\mathbf{B} = B_{z0} \tanh\left(\frac{x}{\ell}\right) \hat{\mathbf{z}},$$

where ℓ is the thickness of the current sheet. In this numerical simulation, we set $\ell = 0.1$ (to satisfy $\ell \ll L_x$). The current sheet is located on the plane $x = 0$. In this numerical simulation, B_{z0} is given as 1.0.

After the initial value of the magnetic field \mathbf{B} has been given, that of the functions A and J can also be obtained from (12e) and (12f) using the analytic solution.

- (2) The initial fluid field is assumed to be:
- (a) the potential fluid is employed as the value of the initial fluid, namely $\Omega = 0$;
 - (b) based on (12c) and the boundary condition of \mathbf{u} , values for Ψ and \mathbf{u} can be obtained and used as the initial values.

As the result of the numerical simulation, the magnetic reconnection simulated and the vector graph of the Hall electric field are given in Figs 4 and 5, respectively. In Fig. 5, two important regions have been marked with ‘N’ and ‘P’ for the sake of convenience in the discussion of the structure of the Hall electric field.

The structure of the Hall electric field in the vicinity of the magnetic reconnection site obtained in the theoretical method can be affirmed in the numerical simulation result of magnetic reconnection shown in Fig. 5. The region marked by ‘N’ denotes the diffusion region of the magnetic reconnection site, where the direction of the vector of the Hall electric field points towards the neutral line of the magnetic field from its two sides. And due to the interaction between the disturbance and the neutral line of the magnetic field, the Hall electric field in the vicinity of the kink of the magnetic reconnection is greater than that in other regions, which can be seen in Fig. 5. What is more exciting in this numerical simulation result is the region marked by ‘P’, where the direction of the vector of the Hall electric field points outwards from the centre of this region, just opposite to that in the diffusion region marked by ‘N’. So, according to the above discussion, it can also be inferred that ions should be generated in the region marked by ‘P’ due to the Hall effects. These results of the numerical simulation accord well with the sketch of the Hall current system made based on the spacecraft observations of the distributions of ions and electrons (see Fig. 2). This kind of structure of the vector graph of the Hall electric field can explain well the decoupling of ions and electrons of the magnetic

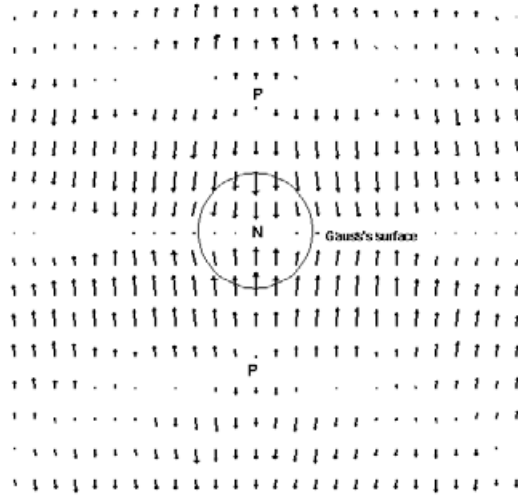


Figure 5. Vector graph of the Hall electric field in the vicinity of the magnetic reconnection site in the region enclosed by the Gauss surface, there is $q_f < 0$. This conclusion means that there will be electrons generated in the diffusion region of the magnetic reconnection site due to the Hall effects. (This figure is a magnified version of the vicinity of the magnetic reconnection site at $t = 10\tau_A$).

plasma in the diffusion region of the magnetic reconnection site due to the Hall effects under the given physical conditions.

7. Conclusion

In the above discussion we have studied the structure of the Hall electric field of a magnetic plasma in the vicinity of the magnetic reconnection site. Based on this, the important conclusion that electrons can be generated in the diffusion region of the magnetic reconnection site due to the Hall effects can be reached. Ions can also be generated in the regions beside the diffusion region based on the numerical simulation result. When the interplanetary shock interacts with the neutral line of the magnetic field, the gradient of the magnetic field in the region near the neutral line is very great. The Hall electric field is relative to the gradient of the magnetic field. Therefore, the Hall effects play an important role in the region where the gradient of magnetic field is great; for example, in the region near the neutral line of the magnetic field. These new finds can explain well the decoupling of ions and electrons of a magnetic plasma due to the Hall effects, and can be supported by the observational results obtained by spacecraft. The diffusion region is important in understanding the mechanism of magnetic reconnection. Of course, there are still many riddles that remain unsolved in this small region concerning the mechanism of the magnetic reconnection.

Acknowledgement

This paper has been supported by the National Natural Science Foundation of China (grant No. 40336053).

References

- Cater, T. A., Yamada, M., Ji, H., Kulsrud, R. M. and Trintchouk, F. 2002 Experimental study of lower-hybrid drift turbulence in a reconnecting current sheet. *Phys. Plasma* **9**, 3272–3288.
- Deng, X. H. and Mastsumoto, H. 2001 Rapid magnetic reconnection in the Earth's magnetosphere mediated by Whistler waves. *Nature* **410**, 557–560.
- Drake, J. F., Swisdak, M., Cattell, C., Shay, M. A., Rogers, B. N. and Zeiler, A. 2003 Formation of electron holes and particle energization during magnetic reconnection. *Science* **299**, 873–877.
- Fu, Z. and Hu, F. Y. Q. 1995 *Numerical Simulation of Space Plasma*. An Hui Province: An Hui Science and Technology Press, p. 380 (in Chinese).
- Fujimoto, M. 2001 Two topics pointing to the importance of resolving Hall effects in reconnection jets. *Proceedings of ISSS-6* 1–3.
- Hesse M. and Birn, J. 2000 Magnetic reconnection: three-dimensional aspects and onset in the magnetotail. *IEEE Trans. Plasma Sci.* **28**, 1887–1902.
- Horbury, T. S., Burgess, D., Franz, M. and Owen, C. J. 2001 Three spacecraft observations of solar wind discontinuities. *J. Geophys. Lett.* **28**, 677–680.
- Ji H., Carter, T., Hsu, S. and Yamada, M. 2001 Study of local reconnection physics in a laboratory plasma. *Earth Planets Space* **53**, 539–545.
- Ma, T. C., Hu, X. W. and Chen, Y. H. 1988 *Principle of Plasma Physics*. An Hui Province: Press of University of Science and Technology in China, pp. 237–238 (in Chinese).
- Ma, Z. W. and Lee, L. C. 2001 Hall effects on the generation of field-aligned currents in three-dimensional magnetic reconnection. *J. Geophys. Res.* **106**, 25 951–25 960.
- Nagai, T., Shinohara, I., Fujimoto, M., Hoshino, M., Saito, Y., Machida, S. and Mukai, T. 2001 Geotail observations of the Hall current system: evidence of magnetic reconnection in the magnetotail. *J. Geophys. Res.* **106**, 25 929–25 949.
- Nagai T., Shinohara, I., Fujimoto, M., Machida, S., Nakamura, R., Saito, Y. and Mukai, T. 2003 Structure of the Hall current system in the vicinity of magnetic reconnection site. *J. Geophys. Res.* **108**, 1357–1366.
- Øieroset, M., Phan, T. D., Fujimoto, M., Lin, R. P. and Lepping, R. P. 2001 *In situ* detection of collisionless reconnection in the Earth's magnetotail. *Nature*, **412**, 414–416.
- Øieroset, M., Lin, R. P., Phan, T. D., Larson, D. E. and Bale, S. D. 2002 Evidence for electron acceleration up to 300 keV in the magnetic reconnection diffusion region of Earth's magnetotail. *Phys. Rev. Lett.* **89**, 195 001–195 005.
- Urrutia, J. M., Stenzel, R. L., Griskey, M. C. and Strohmaier, K. D. 2003 Three-dimensional electron magnetohydrodynamic reconnection, III, Energy conversion and electron heating. *Phys. Plasma* **10**, 2801–2808.
- Vainshtein, S. I., Chitre, S. M. and Olinto, A. V. 2000 Rapid dissipation of magnetic fields due to the Hall current. *Phys. Rev. E* **61**, 4422–4430.
- Wu, S. T., Wang, A. H., Plunkett, S. P. and Michels, D. J. 2000 Evolution of global-scale coronal magnetic field due to magnetic reconnection: the formation of the observed blob motion in the coronal streamer belt. *Astrophys. J.* **545**, 1101–1115.
- Yamada M., Ji, H., Hsu, S., Cater, T., Kulsrud, R., Bretz, N., Jobes, F., Ono, Y. and Perkins, F. 1997 Study of driven magnetic reconnection in a laboratory plasma. *Phys. Plasma* **4**, 1936–1944.
- Yokoyama T. 2000 MHD simulations of magnetic reconnection in solar flares and jets. *Adv. Space Res.* **26**, 511–520.